NUCLEAR ENGINEERING AND DESIGN 25 (1973) 112–125. © NORTH-HOLLAND PUBLISHING COMPANY

EXPERIMENTAL DETERMINATION OF DAMPING IN NUCLEAR POWER PLANT STRUCTURES AND EQUIPMENT

G.C. HART
Department of Mechanics and Structures, University of California, Los Angeles, California 90024, USA

and

P. IBÁÑEZ
Applied Nucleonics Company Inc., Los Angeles, California 90024, USA

Received 28 December 1972

A summary of damping values for structures and equipment obtained in several full-scale dynamic tests performed on a research reactor, three experimental power reactor plants, and a commercial power reactor plant is given. The testing techniques used include steady state shakers, dynamite blasting, and snapback. In an appendix, guidelines are presented for required frequency resolution and record length for damping estimation from blast or snapback records. The influence of system non-linearity upon damping interpretations is also discussed.

1. Introduction

This article presents a summary of the damping obtained from many full-scale tests conducted by UCLA students and faculty. The testing techniques used include steady state shakers, dynamite blasting, and snapback. A detailed description of all noted tests is summarized in a series of technical reports [1–8]*. A summary description of the tests conducted at the Oak Ridge experimental gas-cooled reactor (EGCR) is presented here because of the ability to compare damping obtained using different testing techniques and response levels.

Before presenting the damping summary, it is important to discuss the sensitivity of seismic response to damping uncertainty. First, the sensitivity to response depends upon the type of the response under consideration. In general a structure's maximum acceleration is more sensitive to damping than is the maximum displacement. Also, the sensitivity of response to damping uncertainty decreases as the system damping increases. Stated alternatively, the gradient of the response with respect to damping is greater at lower values of critical damping. The net effect of these observations is that one can take more liberties in estimating modal damping for response purposes as the damping level increases. Consequently, if damping increases as response levels increase, then this increased response will not be as sensitive to damping estimation error as is the low level response [8].

It will be evident from later sections that, as expected, modal damping coefficients for a given system are a function of response level. Some preliminary attempts are taken to quantify this relationship.

The Appendix presents two unrelated but important topics. Considerations which are important in the estimation of damping are discussed first. Guidelines are presented for required frequency resolution and record length for damping estimation from blast or snapback records. The influence of system non-linearity upon damping interpretations is also noted.

* See also other articles in this issue of *Nuclear Engineering and Design.*

2. EGCR damping study

2.1. Description of plant

The EGCR is a combined experimental and power demonstration reactor constructed at Oak Ridge National Laboratory. For technical and economic reasons work on the EGCR project stopped before construction was completed, and the reactor was never op-

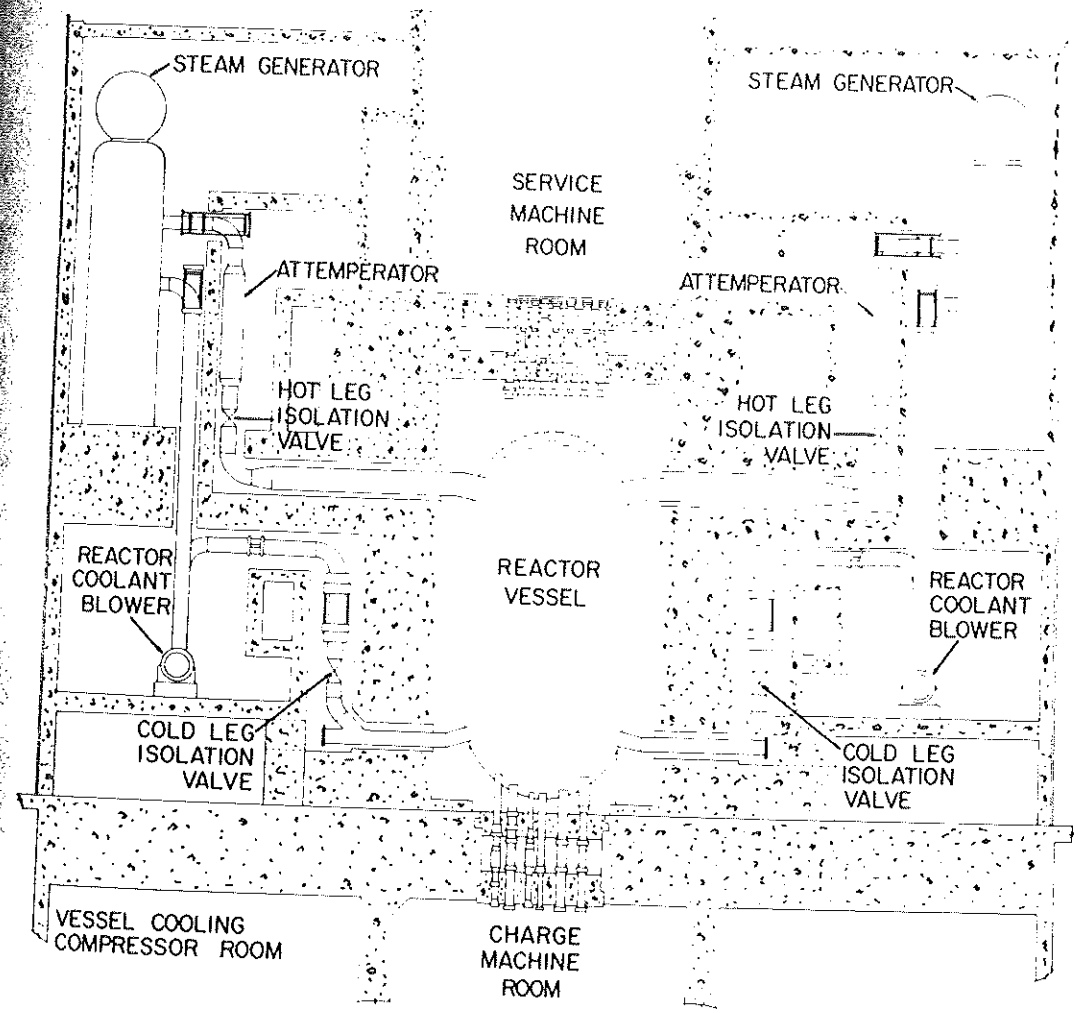

Fig. 1. Schematic representation of EGCR vessel and primary coolant loops.

rated at power. The reactor and containment building have been preserved more or less intact.

The containment structure is a cylindrical concrete structure with an elliptical base and hemispherical dome of steel approximately 200 ft in height. The containment building consists of three main parts. The lower portion (1/3 of the total height) is massive, solid, and buried in the soil. The middle portion, from the ground to the fourth floor, (again about 1/3 of the total height) is roughly symmetrical about the off-center reactor biological shielding, a massive, hollow octagonal cylinder of reinforced concrete. The top 1/3 of the structure is lighter and more flexible, consisting of the two (crane bay) east–west concrete walls inside the steel shell.

A section through this middle 1/3 section is shown in fig. 1 and it indicates the location of primary coolant loop and accelerometer placement locations. There are two steam generators of 9 ft 2 in. dia., 34 ft high, with wall thickness varying between 3–4 in. They are cantilevered off a 9 ft dia. and 9 ft high skirt of 1/2 in. coolant steel. Total weight is 80 ton.

The steam generators are attached to the reactor vessel and coolant blower by pipes typically 24–31 in. dia. with 3/8 – 1 in. thick walls. Typical length varies between 8 and 50 ft. While certain pipes were supported by pipe hangers, no explicit damping devices were installed. The mass of the piping is very

Table 1
(a): Tests conducted at EGCR, 6–7 July 1970.

Test no.	Run no.	Excitation	Charge weight, w (lb)	Depth, d (ft)	Distance, r (ft)	Scale factor, $S = W^{1/3}$	Depth factor, h (ft/lb$^{1/3}$)	Distance Factor, λ (ft/lb$^{1/3}$)	Comments
1	1	Blast	55	50[a]	500	3.8	13.1[a]	131	See note (a)
1	2	Blast	25	25	500	2.92	8.5	171	
1	3	Blast	25	16	500	2.92	5.5	171	
1	4	Blast	60	40	300	3.9	10.2	77	
2	1	Blast	10	7	500	2.15	3.3	232	Shallow blast, crater
2	2	Blast	50	10	650	3.7	2.7	176	Shallow blast, crater
2	3	Blast	10	7	500	2.15	3.3	232	Shallow blast, crater
2	4	Displacement of steam generator							
2	5	Displacement of steam generator							
2	6	Blast	80	60	290	4.3	14	68	
2	7	Blast	160	60	290	5.4	11.2	54	Multiple blast; 2–80 charges in hole 20 ft apart fired simultaneously
2	8	Blast	160	55	290	3.4	10.2	54	Delayed blast; 20–80 charges in hole 20 ft apart fired with a 50 msec delay

[a] 30 lb at a depth of 50ft = 25 lb at a depth of 30 ft. Values obtained by averaging.

(b): Tests conducted at EGCR, 19–24 August 1970.

1	1	Blast	1	60	289	1.00	60.0	289	
1	2	Blast	10	57	289	2.15	26.5	134	
2	1	Blast	10	8	281	2.15	3.72	130	Shallow surface blast
2	2	Blast	100	52	289	4.64	11.2	62.2	
2	3	Blast	600	44	285	8.42	7.5[b]	33.8	200 in each of 3 bore holes detonated simultaneously
2	4	Blast	2000	41	283	12.6	3.5[b]	22.5	1600 in one hole; 400 in second hole simultaneously
3	1	Blast	10	57	251	2.15	26.5	117	
3	2	Blast	100	51	262	4.64	11.0	56.2	
3	3	Blast	600	45	262	8.42	7.70[b]	31.0	200 in each of 3 bore holes: 200 detonated instantaneously, 200 135 msec later, 200 320 msec later
3	4	Blast	2000	54	272	12.6	5.2[b]	21.5	This shot consisted of 1100 in one hole, 675 in second hole, 225 in third hole fired simultaneously

[b] For one hole. If size of charge per hole varied, the largest was used.

much less than that of the steam generator or reactor vessel.

2.2. Description of testing programs

The dynamic response of the EGCR has been investigated by sinusoidal steady state vibrators [4], blast induced ground vibrations [3], and snapback free transient vibrations [3]. These tests provide a unique opportunity to compare the results from these various methods, and to obtain response data at force levels higher than previously possible.

The steady state tests (forced vibration tests) [4] excited the EGCR containment by mounting two eccentric arm vibrators on the operating floor level (floor of service machine room). The maximum eccentric arm used was 15 000 lb in., producing up to 10 000 lb force in the frequency range 0–30 Hz.

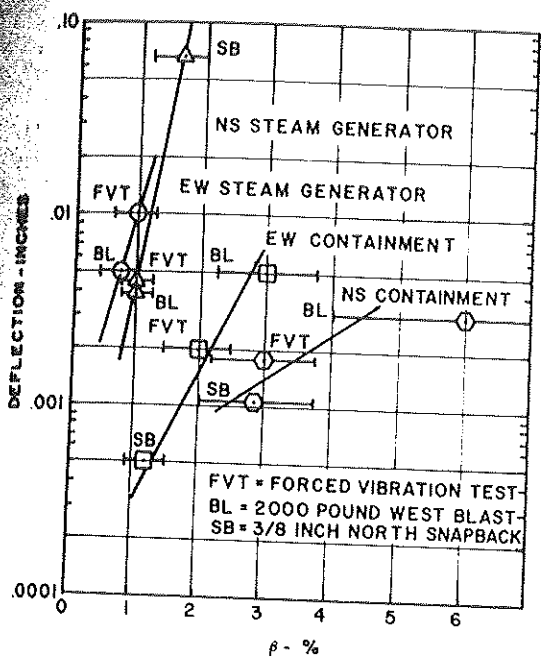

Fig. 2. Variation of effective linear damping with response level.

Tests were carried out with instrumentation on the containment structure and primary coolant loop.

The blast tests were performed by detonating high explosives in the soil near the plant. Tests were performed at varying distances from the structure (25–1000 ft), at varying depths in the soil (0–60 ft), and with varying types and quantities of explosives (10–2000 lb). Structural response was measured with accelerometers reading out on FM tape recorders. Table 1 gives a summary of the blast tests.

For the snapback test a 100 ton hydraulic ram was placed between the steam generator and the containment wall [3]. Displacements up to 3/4 in. were achieved, followed by a sudden release of the steam generator. The primary coolant loop, piping and to a lesser extent the containment structure, then underwent large amplitude free vibrations.

2.3. Observed damping values

During forced vibration testing the steam generators were excited by motion of the containment building. Two steam generator modes of vibration were identified, at 5.8 and 5.92 cps (Hz). Response levels at the top of the steam generator of the order of 10^{-2} in. and 3×10^{-2} G were measured and the damping values were approximately 1% of critical.

As a result of the forced vibration tests, two containment modes were identified – 4.2 and 4.67 Hz. At response levels on the operating floor of 2×10^{-3} in. and $2 \times 10^{-2} G$, damping values were 3 and 2%, respectively.

During blast testing the steam generator modes occurred at 5.6 and 5.7 Hz with damping values of 1.0 and 0.8%. Response levels were of the order of 5×10^{-3} in. and $2 \times 10^{-2} G$. For the containment building the modes were observed at 3.9 and 4.4 Hz with damping values of 6 and 3%. Responses in this case were of the order of 5×10^{-3} in. and $1 \times 10^{-2} G$.

In the snapback tests the predominant north–south steam generator mode (the direction of 'snapping') had a frequency of 5.1 Hz with 1.6–2.0% damping. This occurred at response levels of 0.1 in. and $0.2 G$. The east–west mode was not successfully identified. The containment modes occurred at 3.9 Hz ($\approx$ 2.9%) and 4.5 Hz ($\approx$ 1.3%). Response levels were 10^{-3} in. and $10^{-3} G$.

The EGCR piping response induced by the snapback test was in the $10^{-1} G$ acceleration and the 10^{-2} in. range. Tests indicated a coupled steam generator and piping mode at 5.1 Hz, plus a predominately piping mode at 12 Hz. The piping damping obtained from the tests was 3% critical.

These results are summarized in fig. 2. Here the results for typical tests on four different modes of vibration indicate a tendency for damping to increase as response levels are increased.

3. Summary of other UCLA damping studies

In this section the results from tests on five nuclear power plants are summarized. The plants are: the UCLA research reactor; the experimental gas-cooled reactor (EGCR); the Carolinas-Virginia tube reactor (CVTR); the Enrico Fermi I sodium-cooled reactor; the San Onofre Nuclear Generating Station (SONGS).

The damping estimates for various components of these plants are summarized in table 2. Included is a description of the component, method of excitation, typical observed response levels, the eigenfrequency, and, finally, estimated fraction of critical damping.

Table 2
Summary of damping estimates from vibration tests.

Structure	Excitation	Response levels			Eigenfrequency (Hz)	Damping, fraction of critical
		(in.)	(in./sec)	G		
UCLA research reactor: shielding block, ≃ 20 ft concrete block on soil.	$10^3 - 10^4$ lb Harmonic vibrators	10^{-3}	10^{-1}	10^{-2}	16.20 Rocking on soil (NS, EW)	0.10, 0.07
Fuel element: aluminum plates in a bundle of 11	Electromagnetic vibrator	10^{-3}	10^{-1}	10^{-1}	11.1	0.05
EGCR:						
Concrete containment building, 200 ft high, 30% buried, 100 ft dia., 10^6 slugs	$10^3 - 10^4$ lb Harmonic vibrators	10^{-3}	10^{-2}	10^{-3}	4.7 EW	0.015 – 0.02
					4.2 NS	0.02 – 0.03
					8.2 Torsional	0.02
	Up to 2000 lb detonation at 300 ft	10^{-2}	10^{-1}	10^{-1}	4.5 EW	0.02 – 0.04
					4.0 NS	0.02 – 0.05
Core, cylindrical array of graphite bars 16 in. × 16 in., 20 ft high, 15 ft dia., held top, middle, and bottom. Use of keys causes non-linear response	$10^{-4} - 10^{-3}$ in. on containement due to harmonic vibrators	10^{-3}	10^{-3}	10^{-3}	4.6 EW	0.01
					3.9 NS	0.01 – 0.03
					13.6 EW	0.01
Steam generator, 45 ft high, 9 ft dia., steel pressure vessel with heavy walls (3–4 in.), tube sheets inside, supported on skirt from bottom, several attached pipes, 5000 slugs	10^{-4} in. on containment due to harmonic vibrators	10^{-3}	10^{-2}	10^{-3}	6.0 EW rocking on skirt	0.01
					5.8 NS rocking on skirt	0.01
	Up to 2000 lb detonation at 300 ft. Snapback in NS direction	10^{-2}	10^{-1}	10^{-1}	5.4 EW rocking on skirt	0.02 – 0.03
		10^{-1}	10^{0}	10^{0}	5.1 NS rocking on skirt	0.02 – 0.03

Table 2 (continued)

Table 2 (continued)

Pipe attached to steam generator, 45 ft long, unsupported, 22 in. o.d., 3/8 in. wall	Up to 2000 lb detonation at 300 ft, resulting in $10^{-1}G$, on steam generator, and containment, also during SG snapback	10^{-2}	10^{0}	10^{-1}	12.0 Translational bending perpendicular to pipe	0.02 – 0.03
Concrete exhaust stack, 200 ft high, approximately 30 ft dia.	Ambient	–	–	–	0.9, 4.0	0.01
CVTR:						
Concrete containment building, 114 ft high, 50% buried, 58 ft dia.	10^{3} – 10^{4} lb Harmonic vibrators	10^{-3}	10^{-1}	10^{-2}	8.3 – 9.5 Two closely spaced modes	0.06
Operating floor platform, concrete shield, reactor, and equipment, inside containment. Supported on steel columns. Connected to containment only by fuel transfer canal	10^{3} – 10^{4} lb Harmonic vibrators	10^{-2}	10^{-1}	10^{-2}	4.0 EW translation	0.06
					6.8 NS translation	0.09
					4.0 Torsion	0.06
Stack, 150 ft high	10^{-2} G on containment	10^{-3}	10^{-1}	10^{-1}	20, 24, 40 Higher modes	0.01
Enrico Fermi:						
Steel containment, 100 ft high, 72 ft dia., steel and concrete below grade, 50% buried	Up to 25 lb detonation at 1000 ft	10^{-4}	10^{-2}	10^{-2}	13 – 16	0.06
Intermediate heat exchanger, 24 ft high, 60 in. dia. steel vessel with large diameter (30 in., 12 in.) piping attached. Cantilevered off a skirt, but in close contact with concrete wall		10^{-3}	10^{-2}	10^{-3}	3.0 (Identification of this mode questionable)	0.10
Secondary sodium pump, 19 ft high, 5 ft dia. motor and pump, attached at bottom by plates, and at top by light steel beams. Some attached piping		10^{-3}	10^{-2}	10^{-2}	7.9	0.03
Sodium/water steam generator, 200 in. high, 100 in. dia., many small pipes attached, held top, middle, and bottom by steel frame and struts		10^{-3}	10^{-2}	10^{-2}	15.0	0.10
Fuel transfer machine		10^{-3}	10^{-2}	10^{-2}	8.0	0.06

Table 2 (continued)

SONGS:						
Containment, 140ft dia. steel sphere, continuously supported on lower 30% by below grade concrete cradle, 2×10^6 slugs	$10^3 - 10^4$ lb Harmonic vibrators	10^{-4}	10^{-2}	10^{-4}	4.8 SE rocking on soil	0.16
					7.0 NW rocking on soil	0.18
Pressurizer, 42ft high, 8ft dia. steel pressure vessel, cantilevered off skirt, 10,000 slugs filled with water	$10^{-5} - 10^{-4}$ G on containment due to harmonic vibrators	10^{-3}	10^{-2}	10^{-3}	2.4 NW rocking on skirt	0.02
					2.9 NE rocking on skirt	0.015
	10^{-3} G on containment due to harmonic vibrators	10^{-4}	10^{-2}	10^{-3}	16, 19 Higher models	0.025, 0.010
	Earthquake 9/70 less than $10^{-2}G$ ground motion	$\approx 10^{-1}$	$\approx 10^{0}$	$\approx 10^{-1}$	2.4 NW rocking on skirt	0.02
					2.7 NE rocking on skirt	0.015
Steam generator-coolant pump system (cases of a mode affecting more than one component). Steam generator (SG) is 45ft high, 11ft dia. steel pressure vessel with internal tube sheets, 20 000 slugs. Pump is 25ft high, 9ft dia., 5000 slugs. Both SG and pump connected by large dia. (30 in.) thick wall (3in.) piping with typical lengths of 100in. These pipes also connect them to the reactor vessel. Vertical support by stringers off steel frames. Transverse support comes from the connecting piping. SG also restrained by keys	$10^{-4} - 10^{-3}$ G and 10^{-4} in. on containment due to harmonic vibrators	10^{-3}	10^{-2}	10^{-3}	1.88 Mainly SG	0.015
					2.84	0.015
					3.15 Mainly pump	0.015
					3.95 Piping (?)	0.015
		10^{-2}	10^{-1}	10^{-2}	5.7 Mainly pump	0.015
					8.0 Mainly SG	0.015

Table 2 (continued)

	Earthquake 2/71, $10^{-2}\,G$ ground motion	10^{-1} -10^{-2}	10^{0}	10^{-1}	2.00 Mainly SG	0.04
					2.90	0.03
					3.10 Mainly pump	0.03
					4.00 Piping (?)	0.02
					5.7 Mainly pump	0.02
					8.0 Mainly SG	0.02
Steel containment sphere	$10^{-3}\,G$ on containment due to harmonic tests	10^{-4}	10^{-2}	10^{-3}	11.3	0.05
Reactor Vessel, 38ft high, 13ft dia. thick walled vessel containing reactor core. Supported at three points above center of gravity by keys, 50 000 slugs	$10^{-4}\,G$ on containment due to harmonic vibrators	10^{-4}	10^{-2}	10^{-4}	7.3 (Identification of this mode difficult)	0.015

The values shown are the most recent available, and do not necessarily agree with those quoted in the earlier reports.

Consider first the damping estimates for containments. For the rigid structures generally used as containments, rocking or rocking/translation on the soil generally determines the seismically significant response. In such cases a general trend can be seen as the center of gravity is moved closer to the ground (squatter structures usually have larger dampings). Thus the EGCR has 0.015 – 0.05 damping, the CVTR 0.06, Enrico Fermi 0.06, and SONGS 0.17, which is roughly in order of lowered center of gravities. While diameter of foundation and soil properties are also significant, this trend is qualitatively in accord with the results from foundation/soil interaction theory. Fortunately this theory is able to provide fair estimates of damping, and should be used in design in view of the variability in damping from structure to structure.

Non-linear trends in damping are difficult to determine. Nevertheless, the EGCR containment damping, which ranged from 0.015 – 0.03 at deflection levels of 10^{-3} in., ranged from 0.02 – 0.05 at deflection levels of 10^{-2} in. Thus damping shows a slight tendency to increase over this factor of ten increase in response. Eigenfrequencies changes are not large enough to be significant to damping studies.

The limited data available on exhaust stacks suggest that their damping is low: of the order of 0.01.

The EGCR core graphite, possessing highly non-linear characteristics due to the use of keys is characterized by 0.01 – 0.03 damping at deflection levels of 10^{-3} in. The 140 ft steel containment sphere at SONGS possesses 0.05 damping at 10^{-4} in. deflection level. The CVTR operating platform is characterized by 0.06 – 0.09 damping at 10^{-2} in. response levels.

Perhaps most important to this study is the damping in pressure vessels and associated piping. The EGCR steam generator and the SONGS pressurizer, steam generators, and pumps are characterized by 0.01 – 0.02 damping at $10^{-3} - 10^{-2}$ in. levels and 0.015 – 0.04 damping at $10^{-2} - 10^{-1}$ in. levels. Again, a slight increase of damping is observed over a tenfold increase in response levels. All these components are essentially cantilevered off their support skirt in the first two cases, heavy piping in the others. The steam generator and pumps at SONGS are also held vertically by stringers, and the steam generator is restrained by keys which introduce highly non-linear effects. The SONGS reactor vessel response is not well understood, but one test indicates 0.015 damping at 10^{-4} in. levels.

As a group, the Enrico Fermi experiment shows higher damping: 0.03 – 0.10 at 10^{-3} in. levels. One possible cause is insufficient resolution in the Fourier spectra of the transient time histories which tends to broaden resonant peaks. Alternatively, it is noted that many Fermi components are held at several points as well as cantilevered, and this may lead to higher dampings.

Only limited data is available on piping. One well studied pipe attached to the EGCR steam generator possesses 0.03 damping at 10^{-2} in. levels. In many tests it has been observed that piping tends to move with the pressure vessels. Although this trend is not established for all cases, it suggests that piping is part of the dynamic mode of the vessels and hence should be assigned dampings similar to those seen in vessels. Similarity of construction and materials between pipes and vessels and the limited data available supports this approach.

At this point we mention damping estimates for electrical distribution equipment (transformers, lightning arrestors, switches, disconnects, capacitor banks, etc.) available from vibration tests [9]. In general, response levels have been up to 10^{-1} *G* and 10^{-1} in. All structures tested have resonant frequencies in the range 1 – 10 Hz. Damping estimates run from 0.005 – 0.050, with a slight tendency to increase with increasing response levels.

4. Summary

The estimation of accurate modal damping values for use in reactor design is still not yet possible. However, as the previous sections indicate, it is possible to select, for a particular type of component and expected response level, damping values which represent 'in the ball park estimates' for design considerations. It is suggested that table 2 be used to aid such a selection.

The authors feel that for design purposes, one must distinguish between damping in the elastic response range and the concept of 'equivalent inelastic damp-

ing' for non-linear response calculations. All damping estimates presented are for use in the former category and reflect damping values for response levels well below the structure's natural yield level. In all cases discussed, it is reasonable to assume that the damping values reflect a lower bound to the damping that would be expected at elastic but near yield response levels. The design concept of equivalent inelastic damping is not commented upon in this paper.

Appendix: Damping estimation—computational considerations

A.1. Introduction

The main purpose of this appendix is to investigate the major factors influencing the accuracy with which we can estimate the dynamic properties (period, damping) of structures by the half-power bandwidth method. We emphasize the estimation of damping because period estimation is relatively easy. The mere presence of a spectral peak almost guarantees a good estimate of period. This is due to the fact that spectral peaks tend to be sharp for lightly damped structures and there is little uncertainty as to the frequency corresponding to such a peak. Damping estimation, on the other hand, depends on the exact shape of the spectral peak. It is shown that many factors affect the shape of a spectral peak thus influencing the damping estimator.

In the half-power bandwidth method a standard power spectrum is computed for a blast record and certain peaks are identified which correspond to the various modes of vibration. Once a peak has been selected, its half-power bandwidth is determined and the structural damping associated with this particular mode is computed. This procedure is well known but sometimes does not yield satisfactory results for lightly damped structures. It will be shown below that one plausible explanation for this fact is that insufficient frequency resolution and record length were used to obtain an estimate of damping. In addition spectral smoothing, a standard practice in computing spectra, introduces distortions into the spectral peak resulting in errors in the damping estimator. Also, as we shall see, system non-linearities complicate the estimation process.

The work reported establishes relationships between spectral resolution, record length and the relative error in the damping estimator. These relationships are used to establish the range of structures whose damping can be estimated from blast records.

A.2. Frequency resolution considerations

Shannon's sampling theorem for time domain functions is well known and is one of the basic and most powerful theorems of modern information theory. Briefly stated it is as follows: a band-limited signal containing a maximum frequency f_m, in cycles per second (Hz), must be sampled at a rate greater than or equal to $2f_m$ samples per second (Sps), in order to preserve all of the information contained in the signal. Experience with practical sampled data devices has shown that sample rates of $5f_m$ Sps or greater must be employed where high accuracy for frequencies near f_m is a requirement.

Obviously Shannon's theorem holds not only for functions of time, but for functions of any independent variable. One of the fundamental questions regarding damping estimation concerns the number of frequency domain samples required to accurately define the spectral peak of a damped sinusoid.

To help answer this question, consider the following Fourier transform pair

$$\exp(-\alpha t)\sin\omega_d t \leftrightarrow (\omega_d)/([\alpha^2+\omega_d^2-\omega^2]+j(2\alpha\omega)), \tag{1}$$

where $\alpha \equiv \lambda\omega_0$, $\omega_d \equiv \omega_0\sqrt{(1-\lambda^2)}$, $j \equiv \sqrt{-1}$, λ is the critical damping ratio and ω_0 is the undamped structural natural frequency in radian/sec. The power spectrum of eq. (1) is given by

$$P(\omega)=(\omega_d^2)/((\omega_0^2-\omega^2)^2+4\alpha^2\omega^2). \tag{2}$$

The time domain function in eq. (1) is simply the response of a single-degree-of-freedom oscillator to a unit impulse. Linear, multi-degree-of-freedom systems can be reduced to an equivalent set of uncoupled single-degree-of-freedom oscillators.

In the present study $P(\omega)$ was computed from eq. (2) and the spectral resolution f_r was varied over a wide range. For each resolution, the half-power bandwidth (BW) was determined by linear interpolation. The damping ($\bar{\lambda}$) was then estimated from the

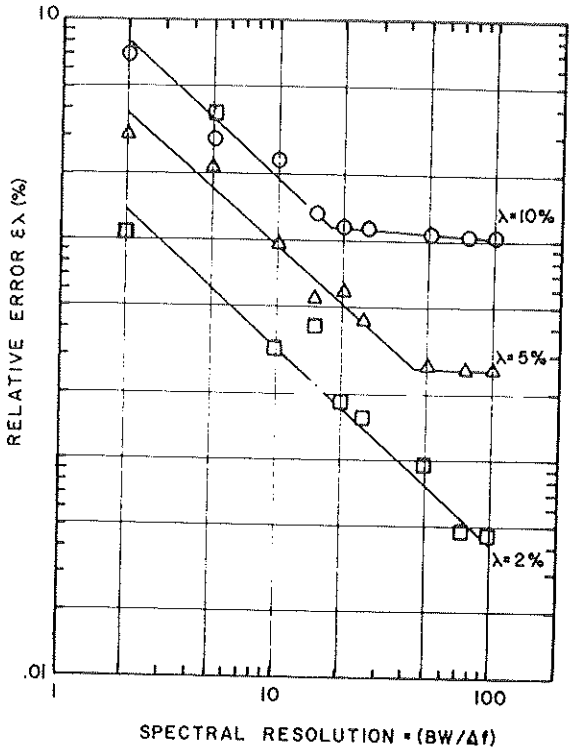

Fig. 3. Unsmoothed damping estimator error vs damping.

following relation

$$f_0 \equiv (\omega_0/2\pi) = \text{natural frequency (Hz)}, \tag{3}$$

$$\text{BW} \equiv 2f_0\bar{\lambda}\,. \tag{4}$$

The per cent relative error between λ, the true damping, and $\bar{\lambda}$, the estimate of damping is

$$e_\lambda = ((\lambda - \bar{\lambda})/(\lambda) \times 100\,. \tag{5}$$

The spectral resolution (f_r) as discussed herein is defined as

$$f_r \equiv \text{BW}/\Delta f \tag{6}$$

where Δ is the frequency domain sample rate in Hz.

The results of this study are presented in fig. 3 where the relative error in the damping estimator is plotted against the spectral resolution f_r. The relative error in unsmoothed spectra has substantial scatter for resolutions below 5. This is due in part to the fact that the central peak may occur between frequency points which tends to reduce the observed spectral peak height. Since the peak height is used to determine the half-power frequencies, an error in peak height carries over to the damping estimate.

Referring to fig. 3, it appears that for reliable damping estimation with an error less than 4% a spectral resolution of about 4 or 5 should be employed, i.e.

$$\Delta f \leqslant 1/5\ \text{BW}\,. \tag{7}$$

The application of this latter equation to practice implies that a preliminary estimate of the structure's natural frequency exists as well as a lower bound damping estimate. Thus, using eq. (4) we obtain BW for use in eq. (7).

The effects of smoothing on damping estimation were studied by computing the power spectrum $P(\omega)$ given by eq. (2) over the same frequency range as in the resolution study. The resulting spectra were then smoothed once by Hanning before determination of the half-power bandwidth. The damping was then estimated as described above. The relative error for the smoothed spectra is consistently higher than for the unsmoothed spectra. That is, smoothing introduces a significant amount of distortion in the shape of a spectrum. Quantitatively, a resolution of 15 for the smoothed spectrum is required to produce the same relative error in the damping estimate as a resolution of 5 for the unsmoothed spectrum.

A.3. Record length considerations

The exact Fourier transform is based on taking the limit of the Fourier integral as t approaches infinity. In estimating the Fourier spectra with a digital computer we must necessarily work with finite record lengths. A computer study was therefore performed to investigate the sensitivity of the damping estimator to record length.

In order to study the effects of a finite record length, we consider the following function

$$h(t) = \exp(-\alpha t)\sin\omega_d t\,[U(t) - U(t-T)]\,, \tag{8}$$

where $\alpha \equiv \lambda\omega_0$, $\omega_d \equiv \omega_0\sqrt{(1-\lambda^2)}$, and T is the record length. If $U(t)$ is the Heaviside unit step function, then taking the Fourier transform of eq. (8) we obtain

$$H(\omega) = \frac{(\omega_d - e^{-\alpha t}e^{-j\omega t}[(\omega_d\cos\omega_d T + \alpha\sin\omega_d T) + j\omega\sin\omega_d T]}{((\omega_0^2 - \omega^2) + j(2\lambda\omega_0\omega))}$$

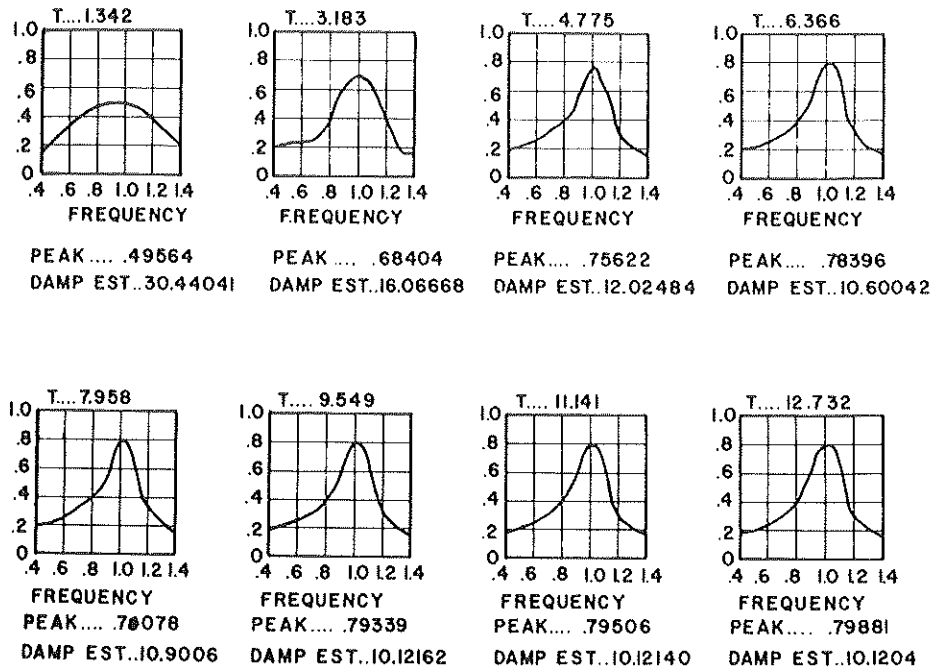

Fig. 4. Unsmoothed modulus of a damped sinusoid for various record lengths computed by the closed form method.

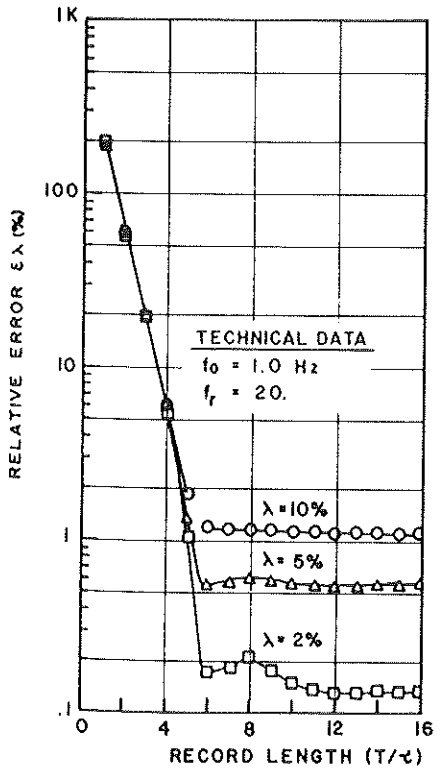

Fig. 5. Error in unsmoothed damping estimator due to finite record length computed by closed form method.

It will be noted that the second term in the numerator grows smaller with increasing record length T. This is due to the term $\exp(-\alpha T)=\exp(-T/\tau)$ when $\tau = 1/\alpha = 1/\lambda\omega_0$. The normalized record length T/τ has damping embedded in its definition and, therefore, is a useful parameter for studying the sensitivity of the damping estimator to record truncation.

Fig. 4 shows plots of the Fourier modulus of $h(t)$ computed from eq. (9) for various values of T/τ. The actual record length T, the modulus peak and the damping estimate are printed near each plot of the Fourier modulus in fig. 4. These moduli were computed for $f_0 = 1.0$ Hz, $\lambda = 0.10$, $\Delta f = 0.01$ Hz, BW = = 0.20 Hz, $\tau = 1.592$ sec and a spectral resolution $f_r = 20$. Fig. 5 is based on the same type of calculation as fig. 4 and shows the relative error in the damping estimator ϵ_λ as a function of T/τ and λ where the damping estimator error is defined as in the resolution study.

We see from the preceding figures that the improvement in damping accuracy and hence the estimator is slowly convergent after T/τ of 5 or 6. Note that since $\tau = 1/\lambda\omega_0$, $T = 5\tau$ implies that

$$T > (1/\pi)\,5/\mathrm{BW}\,, \qquad (10)$$

where BW is in Hz.

A.4. Fast Fourier transform implications

The Cooley–Tukey fast Fourier transform algorithm (FFT) is a rapid numerical procedure for calculating a Fourier transform. In its use, the frequency increment (in Hz) is equal to the inverse of the record length (in sec). Therefore, in the preceding discussions it is apparent that if a blast response is essentially zero after some finite time, it may be necessary to add additional zero response values until the record length is sufficiently long to yield desired frequency resolution.

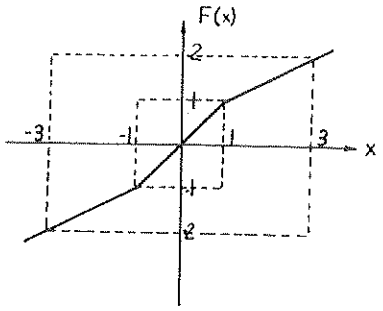

Fig. 6. Non-linear spring stiffness.

A.5. Confusion caused by structural non-linearities

The preceding sections were concerned with considerations which can be readily accounted for. However, as this section shows, the existence of material type non-linearities can result in frequency domain peaks which cloud data interpretations. To show how the non-linear effects cause such peaks in the Fourier moduli of free vibrations, consider a theoretical example. The equation investigated is

$$\ddot{X} + 0.04\dot{X} + f(X) = 0\,, \qquad (11)$$

with $\dot{X}(0) = 0$ = initial velocity, $X(0) = \Delta$ = initial displacement, where $f(X)$ is shown in fig. 6. This implies that the linear damping is 2.00% critical for deflections below unity, and 2.83% critical for very large deflections. Similarly, the eigenfrequency is unity for deflection less than one and 0.707 for large deflections. The response of this bilinear softening system is easily found on the computer; the Fourier moduli are then calculated by the Cooley–Tukey fast Fourier transform.

The graphs in fig. 7 are the Fourier moduli of free transient displacement response, with initial deflection: $\Delta = 1, 2, 5, 20, \to \infty$. The moduli have been normalized by Δ. This figure indicated that non-linear stiffness can cause small peaks to occur in addition to a predominant peak. Note that the position and number of these peaks are not constant, but vary with the level of initial deflection. Furthermore, observe that the width of the predominant peak is also affected by deflection level: the peak

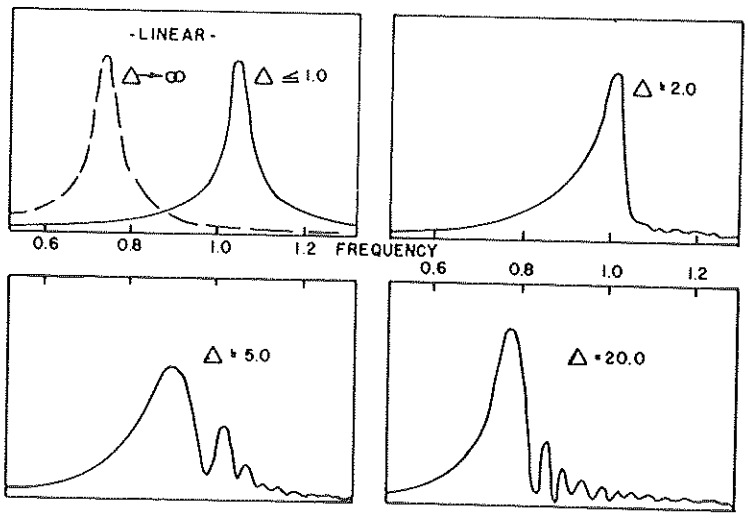

Fig. 7. Fourier modulus of bilinear transient vibration.

from the $\Delta = 5$ release is broader than either the $\Delta = 2$ or $\Delta = 20$ peaks. Thus, the non-linear stiffness may account for some of the variability in linear damping estimates found from experimental data.

All the spurious peaks appear to the right of the main peak, as if when the main peak shifts from 1 to 0.707 Hz it leaves behind it a 'trail of fading memories'. Additional studies confirm the intuitive extension that a hardening spring will produce spurious peaks to the left of the main peak.

References

[1] R. Vasudevan, P. Ibáñez, R. Shanman, R. Matthiesen and C.B. Smith, Modeling the San Onofre Nuclear Generating Station for Seismic Response, UCLA School of Engineering and Applied Science Report, UCLA-ENG-7251, July (1972).

[2] C.B. Smith, P. Ibáñez, R. Matthiesen and R. Vasudevan, Response of San Onofre Nuclear Generating Station to earthquakes, UCLA School of Engineering and Applied Science Report, UCLA-ENG-7151, July (1971).

[3] J. Chrostowski, et al., Simulating Strong Motion Earth quake Effects on Nuclear Power Plants Using Explosive Blasts, UCLA School of Engineering and Applied Science Report, ENG-7119, June (1971).

[4] C.B. Smith and R.B. Matthiesen, Forced Vibration Tests of the Experimental Gas-Cooled Reactor, UCLA School of Engineering and Applied Science Report, 69–42, August (1969).

[5] J.D. Hornbuckle, R.B. Matthiesen and C.B. Smith, Forced Vibration Tests and Analysis of the CVTR Reactor Seismic Response, Amer, Nucl. Soc. Trans. 12 (2) November (1969) 780.

[6] R.B. Matthiesen and C.B. Smith, A Simulation of Earthquake Effects on the UCLA Reactor Using Structural Vibrators, UCLA School of Enigineering and Applied Science Report, NEL-105, October (1966).

[7] P.B. Bleiweis, The Dynamic Response of the Enrico Fermi Nuclear Power Plant During Blasting, M.S. Thesis, University of California, Los Angeles (1970).

[8] R. Vasudevan, P. Ibanez, G. Hart and R.B. Matthiesen, Damping Studies of Nuclear Power Plant Components UCLA School of Engineering and Applied Science Report, In preparation, (1973).

[9] P. Ibáñez, R.B. Spencer and C.B. Smith, Forced Vibration Tests on Electrical Distribution Equipment. Nucl. Eng. Des. 25 (1973).